Passenger Face Recognition Algorithm for Railway Stations Based on Gabor Wavelet and Manifold Learning

Xiang Xu*, Yu Zhang
Railway and Urban Rail Policing College, Zhengzhou Police University, Zhengzhou 450000, China
E-mail of Corresponding Author: xuxiang199506@igit.ac.cn

Keywords: gabor wavelet, manifold learning, face recognition, LPP, LE, LLE

Received: Septeber 23, 2025

To address the low accuracy of traditional station face recognition technology, this paper studies a face recognition algorithm that integrates Gabor wavelet and manifold learning, and constructs a station passenger face recognition system based on this improved algorithm. The algorithm utilizes Gabor wavelet transform to enhance multi-scale and multi-directional image features, employs manifold learning methods such as local linear embedding and Laplacian feature mapping to reduce feature dimensionality, and completes feature extraction and classification through local preservation projection. Results show that on the AR, ORL, and YALE datasets, the algorithm achieves a recognition accuracy of 97%, with an area under the precision-recall curve (AUC) of 0.87. Even with a small number of training samples, it maintains a recognition rate above 93% and a shorter running time, both superior to comparative algorithms. In system application analysis, its mean absolute error is stable between 1.14 and 4, with a maximum absolute percentage error of 5.65%, significantly outperforming traditional LPP and ML-LPP algorithms. The proposed algorithm and system effectively improve station security check efficiency and recognition reliability, providing a new technical solution for public transportation security.

Povzetek: Algoritem z Gaborjevimi valčki in učenjem mnogoterosti doseže ~97 % točnost ter bistveno izboljša zanesljivost in učinkovitost varnostnih pregledov na postajah.

1 Introduction

The accelerated growth of public transportation has facilitated a significant increase in the convenience of travel for individuals. This is evidenced by the substantial daily influx of passengers at transportation hubs, particularly during holidays, when the number of travelers has reached a remarkable level [1, 2]. The use of manual security checks, a traditional security check method, not only increases the work pressure of station staff, but also leads to omissions in security check work when staff are fatigued [3, 4]. To ensure the good operation of the station, the station has started using Facial Recognition Systems (FRS) for security checks. While improving the speed of security checks, it also helps to maintain order in public places [5]. However, when traditional Facial Recognition Technology (FRT) is applied to stations, due to the complex environment of the station, the system exposes shortcomings such as low work efficiency and low recognition accuracy. This system not only fails to improve the security inspection speed of the station, but also increases the workload of station staff. In this context, to improve the efficiency and accuracy of station security checks, the study proposes to improve traditional face recognition algorithms by combining Gabor Wavelet Algorithm (GW) with Manifold Learning Algorithm (ML). Meanwhile, passenger FRS suitable for complex station situations is constructed. It is hoped that this new system can improve the accuracy of passenger facial recognition at stations, thereby improving the speed of station security checks and aiding for the further development of public transportation.

The content includes five parts. The first part is the background introduction of FRT. The second part is an overview of the current research status of FRT. The third part is the construction of the station FRS based on GW and ML. The fourth part is the performance analysis and practical application effect analysis of the proposed station FRS. The fifth part is the summary of the full text, and points out the shortcomings of the research. The terms and their abbreviations in the study are shown in the Table 1.

Table 1: Abbreviations

Terminology	Abbreviation
Facial Recognition Systems	FRS
Facial Recognition Technology	FRT
Gabor wavelet algorithm	GW
Manifold learning algorithm	ML
electroencephalogram	EEG
Locality Preserving Projections	LPP
Locally Linear Embedding	LLE
Laplacian Eigenmaps	LE

2 Related works

With the continuous improvement of science and technology, the methods for identifying people's identities are gradually diversified, and FRT is widely used in many fields. Many scholars use various new technologies and methods to improve the accuracy of facial recognition. Otani and Ogawa proposed a deep learning FRS based on artificial intelligence to address the issue of low accuracy of traditional FRT for wildlife recognition. Empirical analysis of the actual application effect of this system showed that it could improve the accuracy of wild macaque image recognition [6]. The Wang team proposed a robust block diagonal dictionary learning FRT method based on virtual samples, which solves the problem of noise and outliers reducing face recognition accuracy. Comparative analysis showed that this technology could effectively reduce the impact of noise and outlier, thus improving the accuracy of face recognition [7]. Wang et al. proposed an FRT that integrates multi-view low rank representation methods to address the issue of low discrimination ability for specific local structures in multi-view face recognition. Comparative experiments have shown that this technology has improved the recognition accuracy of different views [8]. Chen's team proposed a neighborhood weighted average-based FRS to address the significant impact of factors such as occlusion and facial expressions on the accuracy of traditional FRT. This system could effectively improve the accuracy of face recognition under adverse factors [9]. Sun et al. proposed an FRS that combines near-infrared and ordinary visible light to address the difficulty of facial recognition caused by the use of ordinary visible light. After conducting experiments on traditional FRS, it was demonstrated that the system can improve the accuracy of nighttime facial recognition [10].

Due to the strong visualization processing ability of ML for high-dimensional linear and nonlinear data, the algorithm can be seen in various fields. Wan's team put forward a fading poetry classification method based on manifold learning and adaptive neighborhood selection to address the issue of data fading during Electroencephalogram (EEG) signal analysis. The results indicated that this method could effectively improve the accuracy of fading data classification [11]. Cui et al. raised a manifold learning monitoring method based on non parametric strategies to address the issue of insufficient fault detection performance in industrial process monitoring. This method had the feasibility and effectiveness of fault detection [12]. To solve the problem of small sample size in the process of data dimensionality reduction, Ran et al. put forward an ML that combines unified criteria with matrix function. Compared to existing methods, this algorithm could effectively solve small sample size problems and reduce computational complexity [13]. Dornaika proposed a manifold learning method that combines computational embedding cascading to address the impact of high-dimensional data on machine learning performance. This method had advantages in improving ML performance [14]. Duan et al. raised a sparse discriminative learning feature extraction method based on local manifold learning to address the issue of low ability to extract high-dimensional data features from hyper-spectral images. This method significantly improved the feature extraction ability [15].

In summary, through the continuous innovation of FRT by many scholars, ML has also been applied in various fields, and the potential research value of combining the two is enormous. However, there are still a few scholars who have studied the combination of the two. To address the research gap, a face recognition algorithm based on GW and ML is proposed, and a station FRS is constructed based on this algorithm. It is expected that this study can improve the accuracy of facial recognition in stations and provide technical support for the good construction of public services.

3 Construction of station FRS based on GW and ML

People's lives are becoming increasingly convenient, with an increasing number of people traveling during holidays and a sharp increase in the pressure of manual security checks. To improve the speed of station security checks, an increasing number of stations are utilizing FRS technology. However, the practical application of traditional FRT in stations is not effective, often resulting in the inability to provide passenger facial information and low recognition accuracy. Based on the above research background, this chapter proposes to use GW and ML to improve traditional face recognition algorithms and constructs station passenger FRS.

3.1 A station face recognition algorithm based on ML fusion

The face recognition algorithm is a recognition algorithm that detects facial images, determines key facial features, and feeds them back into the backend after a series of processing. The two-dimensional Locality Preserving Projections (LPP) algorithm is one of the traditional face recognition algorithms, which can directly extract effective features from the facial image matrix and achieve the goal of facial recognition [16, 17]. The workflow of this algorithm is Figure 1.

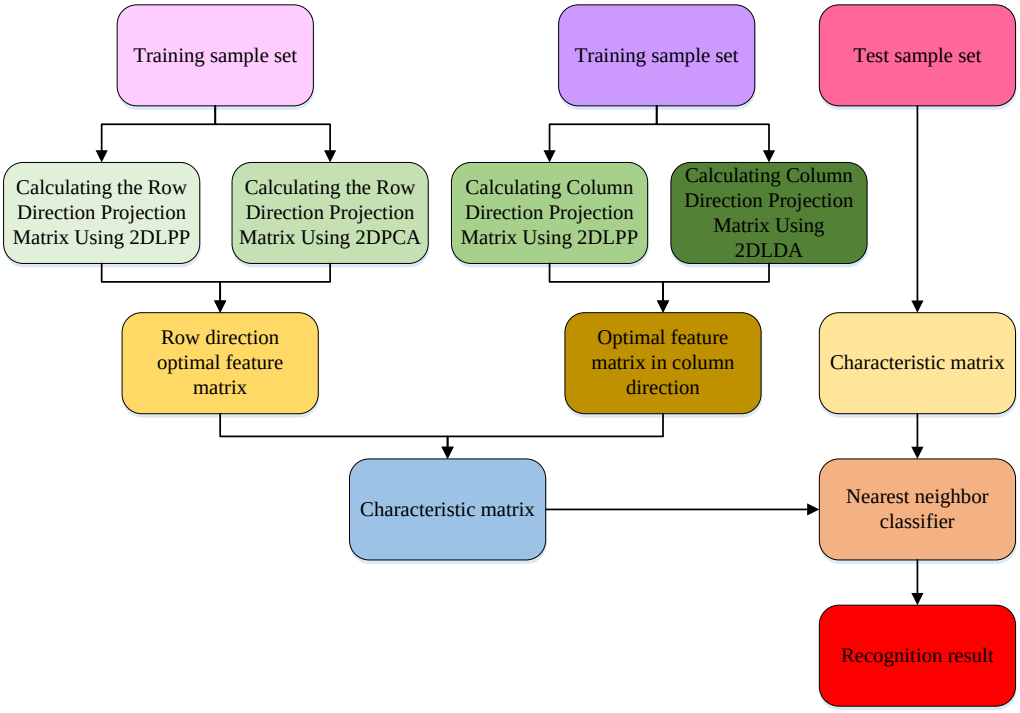

Figure 1: Feature extraction process

From Figure 1, when using this algorithm for feature extraction, it is necessary to calculate the row and column direction projection matrices of the data. After obtaining the optimal feature matrices for row and column directions, they are combined into feature matrices. At the same time, another feature matrix is obtained based on the data in the test sample set, and the final result is output through the selection of the nearest neighbor classifier. During the algorithm operation, the calculation formula for the row direction projection matrix is expressed in equations (1), (2), (3), and (4).

$$G = E\left[\left(X - EX\right)^T \left(X - EX\right)\right] = \frac{1}{M}\sum_{i=1}^{M}\left(x_i - \bar{x}\right)^T \left(x_i - \bar{x}\right) \quad (1)$$

In equation (1), E represents identity matrix. T represents the transposition of the matrix. G is the covariance matrix. X represents the projection matrix. x_i is the sample. i represents the number of samples. $\bar{x}$ is the sample mean. M represents the sum of samples.

$$J\left(A\right) = tr\left\{E\left[Y^1 - EY^1\right]\left[Y^1 - EY^1\right]^T\right\} = tr\left\{E\left[XA - EXA\right]\left[XA - EXA\right]^T\right\} = A^T GA \quad (2)$$

In equation (2), $J\left(A\right)$ is the total sample divergence matrix. Y^1 represents the matrix after dimensionality reduction. A refers to any matrix. A^T represents the transpose of any matrix.

$$\begin{cases} \max\limits_{A}\left(A^T GA - A^T X^T \left(L \otimes I_m\right) XA\right) \\ s.t. A^T X^T \left(D \otimes I_m\right) XA = 1 \end{cases} \quad (3)$$

In equation (3), I_m represents the identity matrix with rank m. X^T is the transposition of the projection matrix. D refers to the coefficient matrix. L is the identity matrix.

$$\left(GA - X^T \left(L \otimes I_m\right) X\right) A = \lambda X^T \left(D \otimes I_m\right) X \quad (4)$$

In equation (4), λ represents the eigenvalues of the matrix. By solving equation (4), the optimal feature matrix in the row direction can be obtained. The calculation formula for the column direction projection matrix is equations (5), (6), (7), and (8).

$$\begin{cases} \min\limits_{A} ZX^T \left(L \otimes I_n\right) \\ ZX^T \left(D \otimes I_n\right) XZ^T = 1 \end{cases} \quad (5)$$

Z in equation (5) represents the projection matrix. Z^T represents the transposition of the projection matrix. I_n represents the identity matrix with rank n.

$$F\left(Z\right) = \max_Z \frac{tr\left(S_B\right)}{tr\left(S_W\right)} = \max_Z \frac{ZG_B Z^T}{ZG_W Z^T} = \max_Z ZG_W^{-1} G_B Z^T \quad (6)$$

In equation (6), $F\left(Z\right)$ represents the objective function. S_B represents the inter class divergence matrix. S_W refers to the intra-class divergence matrix. G_B and G_W are transformation matrices. G_W^{-1} represents the inverse matrix of the transformation matrix.

$$\begin{cases} \max\limits_{Z}\left(ZG_W^{-1} G_B Z^T - ZX^T \left(L \otimes I_n\right) XZ^T\right) \\ s.t. ZX^T \left(D \otimes I_n\right) XZ^T = 1 \end{cases} \quad (7)$$

The equation (7) is simplified based on generalized eigenvalues to equation (8).

$$\left(G_W^{-1} G_B - X^T \left(L \otimes I_n\right) X\right) Z^T = \lambda X^T \left(D \otimes I_n\right) XZ^T \quad (8)$$

By using equation (8), the optimal feature matrix in the column direction can be obtained, which is combined with the optimal feature matrix in the row direction to ultimately obtain the feature matrix on the training

sample set. It is processed with the feature matrix on the test sample set through a classifier to obtain the final recognition result. However, this algorithm is greatly affected by the sample data size and has insufficient anti-interference ability. When the environment in the station is complex, it has a significant impact on the accuracy of algorithm recognition. Therefore, in response to the shortcomings of traditional face recognition algorithms in both aspects, ML and GW are proposed to improve them. ML is one of the pattern recognition algorithms. The core work content is to restore the data in the high-dimensional space to the low dimensional manifold, and meanwhile embed the mapping to preserve the data characteristic attributes. The aim is to achieve the purpose of data visualization, which is often used to find the potential structure of data. When using this algorithm for facial recognition of station passengers, a series of facial images in the station are actually data points in high-dimensional space. It utilizes manifold algorithms to achieve data dimensionality reduction, preserve facial image structural features, and provide data support for subsequent facial feature extraction. The dimensionality reduction effect of the manifold algorithm is Figure 2.

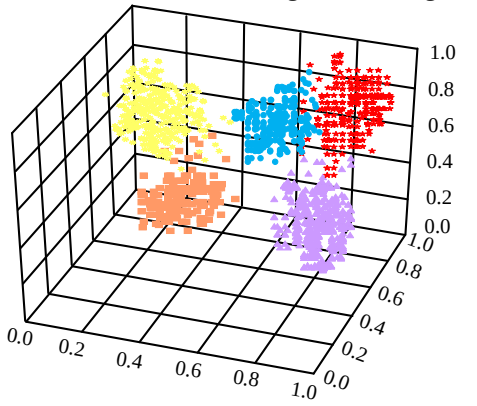

(a) High dimensional data distribution

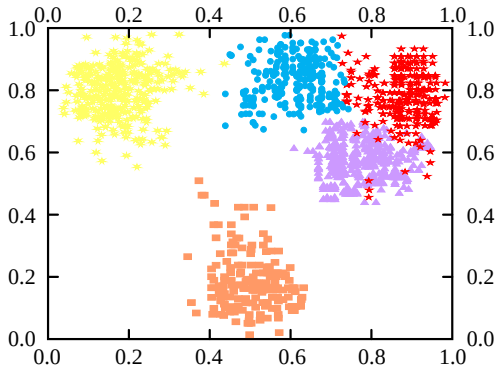

(b) Data distribution after dimensionality reduction

Figure 2: Schematic diagram of the dimension reduction of the manifold algorithm

The manifold algorithm is divided into linear manifold and nonlinear manifold. The nonlinear manifold algorithm is further divided into global nonlinear manifold and local nonlinear manifold, and the latter is studied and used for station face recognition. In the process of data dimensionality reduction using the local nonlinear manifold algorithm, Locally Linear Embedding (LLE) and Laplacian Eigenmaps (LE) are used [18,19]. The calculation principle of LLE is to assume that a sample data point has a linear relationship with nearby small range data. After dimensionality reduction, the dimensionality of the reduced sample data point and the nearby data point still maintain the same linear relationship. This linear relationship does not affect the data far from the sample data points and reduces the complexity of dimensionality reduction. The calculation process diagram is shown in Figure 3.

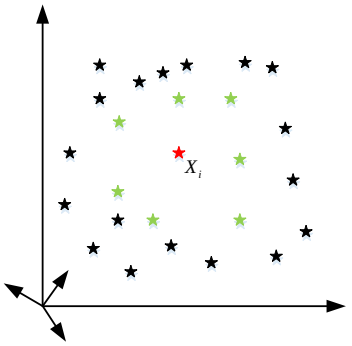

(a) Select Nearest Neighbors

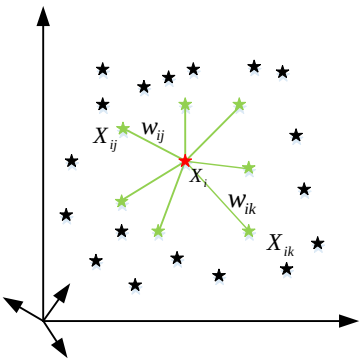

(b) Building linear relationships

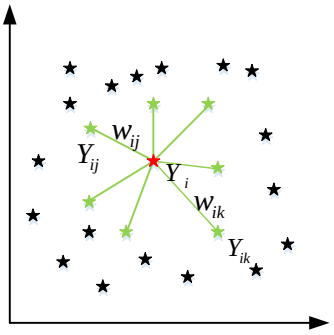

(c) Embedding dimensionality reduction coordinates

Figure 3: Schematic diagram of the LLE calculation flow

In Figure 3, X_i represents high-dimensional sample data points. X_{ik} and X_{ij} are the data points closest to sample data K. Y_i, Y_{ij} and Y_{ik} are corresponding data points in low dimensional coordinates, respectively. w_{ij} and w_{ik} represent the approximate weights for dimensionality reduction of high-dimensional data X_i. In the process of dimensionality reduction calculation, selecting the appropriate K-nearest neighbor is the key. When the nearest neighbor range is too small, many data components are not connected. When the nearest neighbor range is too large, it may lead to unstable connectivity. The basic principle of LE is to construct relationships between data points based on local similarity of sample data points, and combine them with LLE to select moderate K-nearest neighbors for dimensionality reduction calculations. The construction of a suitable nearest neighbor information graph is shown in Figure 4.

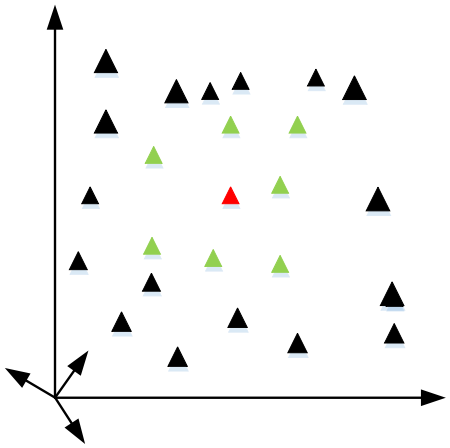

(a) Raw data points

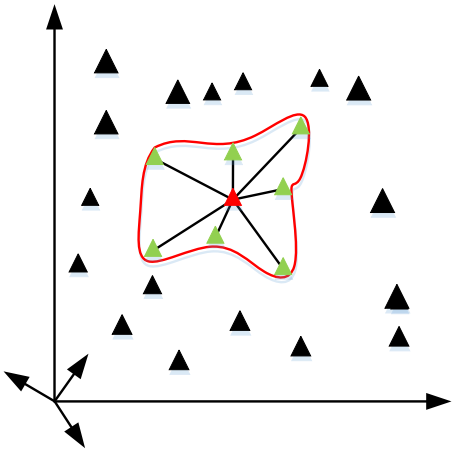

(b) *K*-Nearest Neighbor Point Reconstruction

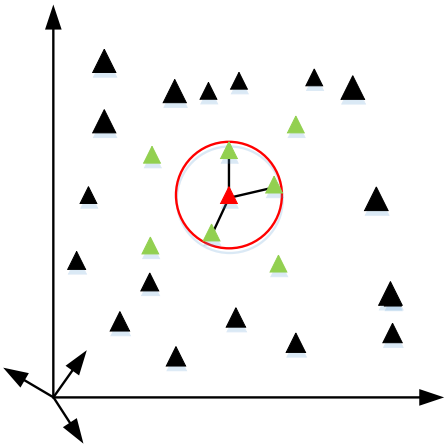

(c) ε- Nearest Neighbor Point Reconstruction

Figure 4: Schematic of proximity information

From Figure 4, LE converts the K-nearest neighbor linear relationship in high-dimensional data into the ε-nearest neighbor linear relationship. The mathematical expression for the conversion process is expressed in equations (9), (10), and (11).

$$\begin{cases} L_1 \overset{\Delta}{=} D_1 - W \\ D_{ij} = \sum_j w_{ij} \end{cases} \tag{9}$$

In equation (9), L_1 is the Laplace calculation definition. D_1 is a diagonal matrix. W represents the approximate weight matrix. D_{ij} is the element in the diagonal matrix D_1.

$$\begin{cases} \left\| x_i - x_j \right\|^2 < \varepsilon \\ w_{ij} = e^{-\frac{\left\| x_i - x_j \right\|^2}{t}} \end{cases} \tag{10}$$

In equation (10), x_i and x_j are data points in high-dimensional data. ε represents the nearest neighbor range. t is a constant.

$$\sum_{ij} \left\| y^{(i)} - y^{(j)} \right\|^2 w_{ij} = tr(F^T LF) \tag{11}$$

In equation(11), $y^{(i)}$ and $y^{(j)}$ are the data points after dimensionality reduction. F represents the embedding matrix. LF is a generalized feature vector. ML and LPP algorithms have similar attributes. Using ML to improve the LPP algorithm, the improved algorithm has good connectivity, and the use of dimensionality reduced facial image sample data in the algorithm can improve facial recognition accuracy.

3.2 Station FRS based on the Gabor-ML-LPP

The anti-interference ability of traditional face recognition algorithms is weak. Popular learning algorithms do not have strong anti-interference capabilities. Therefore, in stations with high pedestrian

traffic and complex environments, their recognition performance is limited. Therefore, the study proposes to use GW to further improve the improved face recognition algorithms mentioned above. GW is similar to the visual stimulus response in the human visual system, and can directly perform two-dimensional wavelet filtering on facial images. When extracting target images, this algorithm has superiority in local space and frequency domain information [20]. Moreover, the influence of external factors such as light in the environment on this algorithm can be ignored, so this algorithm has great advantages in image feature extraction and is widely used in the field of image recognition. The preliminary improvement of the station face recognition algorithm combined with GW enhances the anti-interference ability of the station face recognition algorithm, thereby improving the accuracy of station passenger facial recognition. GW can accurately capture the spatial frequency and structural features of multiple directions in the local area of the target image during image conversion. GW two-dimensional kernel function can enhance the edge features in the target image, which not only enhances the eye, mouth, and nose features in facial images, but also enhances features such as wrinkles and scars. The two-dimensional kernel function expression of GW is equation (12).

$$\begin{cases} \psi \vec{x} = \dfrac{\left\|\vec{k}\right\|^2}{\sigma^2} \exp\left(-\dfrac{\left\|\vec{k}\right\|^2 \left\|\vec{x}\right\|^2}{2\sigma^2}\right)\left[\exp(i\vec{k}\vec{x}) - \exp\left(-\dfrac{\sigma^2}{2}\right)\right] \\ \vec{k} = \begin{pmatrix} k_v \cos\varphi_u \\ k_v \sin\varphi_u \end{pmatrix} \end{cases} \tag{12}$$

In equation (12), $\vec{x}$ is the image coordinate of the specified position. $\vec{k}$ represents the center frequency of the Gabor wavelet filter. σ is the Gabor wavelet frequency bandwidth constant. φ_u represents the sampling direction, and u is the direction label. $\sin\varphi_u$ and $\cos\varphi_u$ are sine wave function and cosine plane wave respectively. k_v is the Gaussian envelope function, and its calculation formula is equation (13).

$$k_v = k_{\max} / f^v = 2^{-\frac{v+2}{2}} \tag{13}$$

In equation (13), $k_{\max}$ represents the maximum center frequency of the filter. f^v is a filter fixed to a specific frequency band. v represents the velocity of the wave. The two-dimensional Gabor wavelet filter function has real and imaginary parts, and the expression of the real part function is equation (14).

$$\mathrm{Re}\left(\psi\left(\vec{x}\right)\right) = \frac{\left\|\vec{k}\right\|^2}{\sigma^2} \exp\left(-\frac{\left\|\vec{k}\right\|^2 \left\|\vec{x}\right\|^2}{2\sigma^2}\right)\left[\cos(i\vec{k}\vec{x}) - \exp\left(-\frac{\sigma^2}{2}\right)\right] \tag{14}$$

The expression of the imaginary part function is equation (15).

$$\mathrm{Im}\left(\psi\left(\vec{x}\right)\right) = \frac{\left\|\vec{k}\right\|^2}{\sigma^2} \exp\left(-\frac{\left\|\vec{k}\right\|^2 \left\|\vec{x}\right\|^2}{2\sigma^2}\right)\left[\sin\left(\vec{k}\vec{x}\right)\right] \tag{15}$$

Finally, the recognition result of the target image can be obtained by convolution operation between the Gabor wavelet kernel function and the target image, and its calculation formula is equation (16).

$$W_{uv}(z) = I(z) * \psi_{uv}(z) \tag{16}$$

In equation (16), $W_{uv}(z)$ represents the target image recognition result. $I(z)$ is the target image. $\psi_{uv}(z)$ represents the Gabor wavelet kernel function of the target image. Combining two-dimensional Gabor wavelet with LPP, the image feature extraction process is shown in Figure 5.

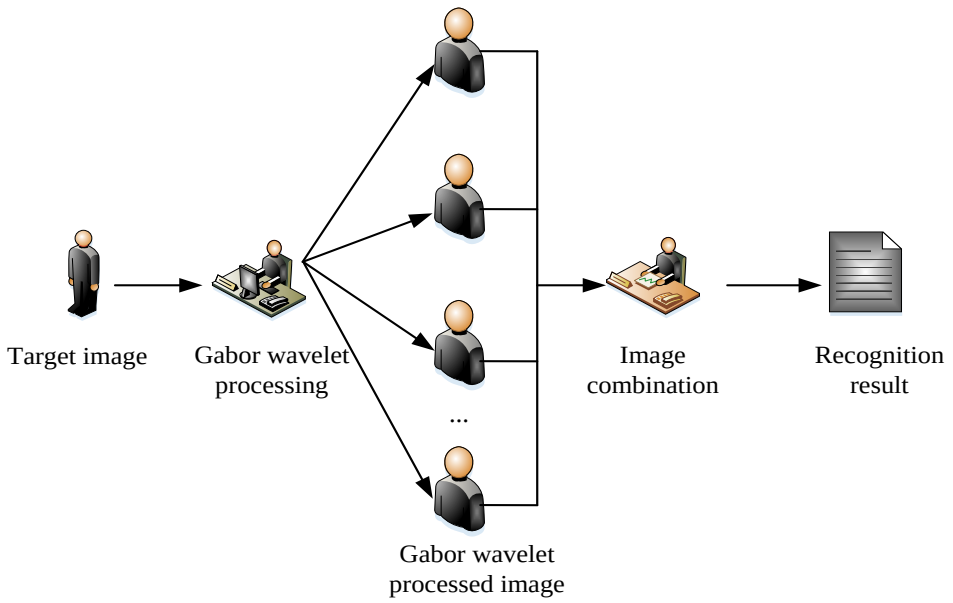

Figure 5: Feature extraction process of fused Gabor wavelets

In Figure 5, the Gabor wavelet filter is first used to process the target image to obtain multi-angle and multi-directional feature images. Then these images are recombined through the operation rules of adding in the same direction and angle. Subsequently, feature extraction is performed on the combined feature images, selecting the optimal features and outputting the recognition results. GW has strong image recognition ability, which can be ignored due to the influence of sample size. It also has strong anti-interference ability, which means it can still maintain high image recognition accuracy in complex environments. Therefore, this algorithm can be used to study the preliminary improvement of station passenger face recognition algorithms to compensate for the shortcomings of station passenger face recognition algorithms. After two improvements, the face recognition algorithm can improve the accuracy of facial recognition for station passengers. After integrating GW, the station FRS workflow diagram is shown in Figure 6.

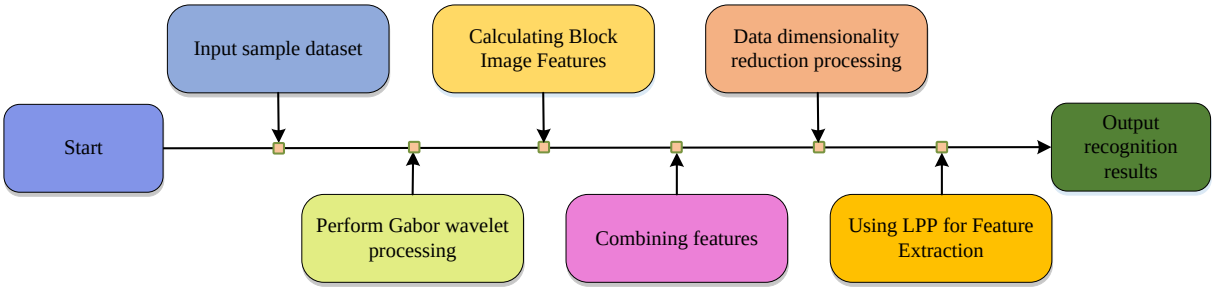

Figure 6: Workflow of the station face recognition system

In Figure 6, due to the inability of GW to perform dimensionality reduction on high-dimensional data, the dimensionality of the feature map data after Gabor wavelet processing remains unchanged. Therefore, after Gabor wavelet processing of facial images in the station, ML is used for data dimensionality reduction processing. Subsequently, the LPP traditional face recognition algorithmis used to extract and recognize facial image features again, and the final facial recognition results are output.

4 Performance testing of improved algorithms and empirical analysis of station passenger FRS

To validate the proposed face recognition algorithm for station passengers based on GW and ML, the study conducts algorithm performance comparison experiments on AR datasets with sufficient facial data samples. The experiment evaluates the performance of the algorithm based on indicators such as running time, recognition rate, accuracy, accuracy-recall rate. Then, to verify the actual application effect of the station passenger FRS, the study uses the average absolute error, the maximum absolute percentage error, the recognition rate, etc. as evaluation indicators to analyze the system application effect.

4.1 Comparative performance testing of gabor-ML-LPP face recognition algorithms

To conduct performance comparison tests on Gabor-ML-LPP, a face recognition algorithm that has undergone two improvements. This study uses traditional human LPP and the improved ML-LPP as the control group. Using these three face recognition algorithms to recognize and detect facial information data in the AR dataset, the experimental results of the algorithm's runtime and recognition rate are shown in Figure 7.

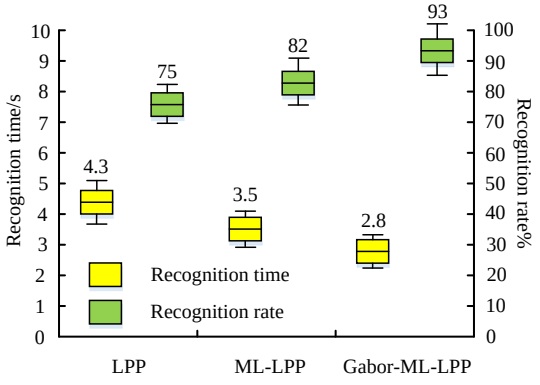

(a) The number of training samples is 4

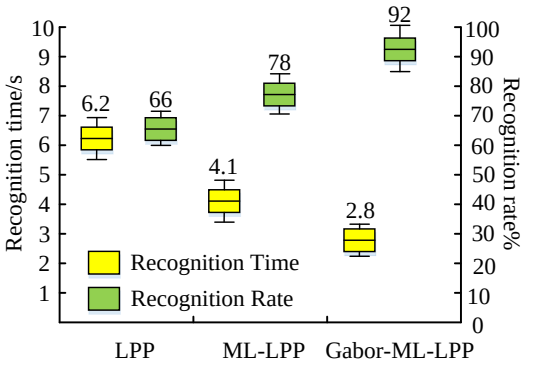

(b) The number of training samples is 6

Figure 7: Running time and recognition rates of the three algorithms

In Figure 7(a), when the number of training samples is 4, the running time and recognition rate of LPP are 4.3s and 75%, ML-LPP is 3.5s and 82%, and Gabor-ML-LPP is 2.8s and 93%. When the number of training

samples is 6, the LPP is 6.2 seconds with 66%, ML-LPP is 4.1 seconds with 78%, and Gabor-ML-LPP is 2.8 seconds with 92%. Based on Figure 7(a) and Figure 7(b), Gabor-ML-LPP performs the best in terms of runtime and recognition rate, and its impact is not significant with the number of samples. The results of multiple experiments using these three types of FRTs are displayed in Figure 8, and the algorithm is evaluated using accuracy and accuracy-recall curves.

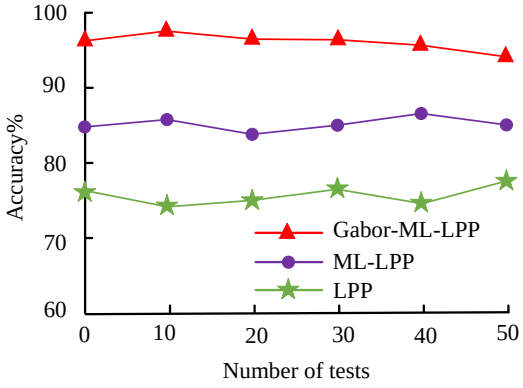

(a) Accuracy curve

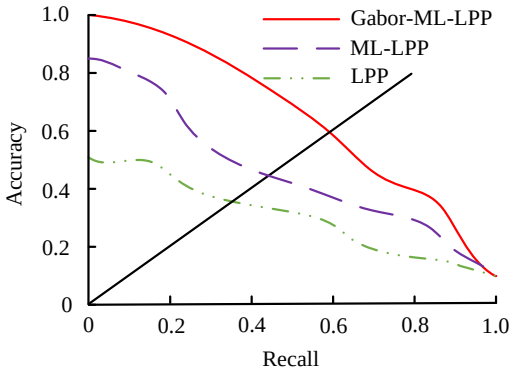

(b) Accuracy recall curve

Figure 8: Accuracy and accuracy-recall curves of the three algorithms

In Figure 8(a), in 50 experiments, the accuracy of Gabor-ML-LPP remains above 90%, with a maximum value of 97%. ML-LPP remains in the range of 80% - 90%, with a maximum value of 86%. The LPP ranges from 70% to 80%, with a maximum value of 76%. In Figure 8(b), the area value under the accuracy-recall curve of Gabor-ML-LPP is 0.87, which is significantly greater than the other two algorithms. A larger area value indicates better algorithm performance. By comparing the results of the above two indicators, Gabor-ML-LPP is superior to the other two algorithms. Subsequently, iterative experiments are conducted using Gabor-ML-LPP, ML-LPP, and LPP algorithms, and the experimental results are shown in Figure 9.

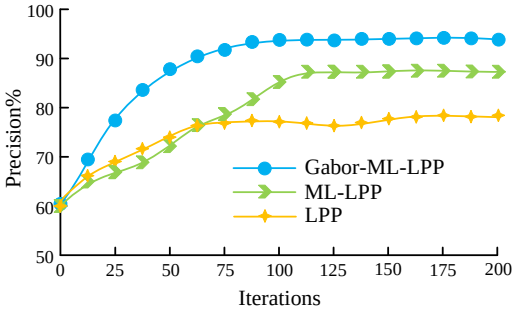

(a)Precision curve

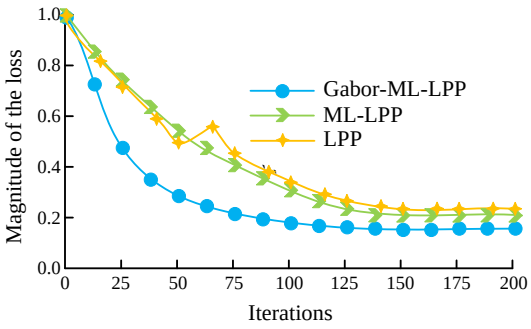

(b)Loss value curve

Figure 9: Accuracy and loss values for the three algorithms

In Figure 9(a), after 200 iterations, the accuracy of Gabor-ML-LPP remains stable at 94%, ML-LPP remains stable at 88%, and LPP remains stable at 79%. Among them, Gabor-ML-LPP has the highest accuracy and fastest convergence speed, which is superior to the comparison algorithm. After 200 iterations, the loss value of Gabor-ML-LPP remains at 0.18, ML-LPP remains at 0.21, and LPP remains at 0.22. Gabor-ML-LPP has the lowest loss value and is superior to the comparison algorithm. In summary, the performance of Gabor-ML-LPP is excellent in all the experimental evaluation indicators mentioned above, and it is expected that this algorithm can improve the accuracy of station passenger FRS. To verify the comprehensive performance of the designed algorithm, the study conducts training on the AR data set, and calculates the average training time, average classification time and best recognition rate of the three algorithms, and reference [4] and reference [5] respectively. The results are shown in Table 2.

Table 2: Average training time, average classification time and best recognition rate of different algorithms

Algorithm	Average training time (s)	Average classification time (s)	Best recognition rate (%)
LPP	3.09	2.94	93.32
ML-LPP	2.81	2.85	94.75
References [4]	1.52	1.47	97.14
References [5]	1.68	1.32	97.86
Gabor-ML-LPP	0.49	0.68	98.68

From Table 1, the average training time of Gabor-ML-LPP is 0.49s, the average classification time is 0.68s, and the best recognition rate is 98.68%. The training time and classification time of the designed method are obviously smaller than other methods, and the optimal recognition rate is higher than other methods. The results show that Gabor-ML-LPP has better recognition performance and computational efficiency, which shows that the algorithm realizes the completeness of feature extraction and ensures the timeliness in classification ability.

4.2 Practical application analysis of FRS for station passengers

LPPFRS and ML-LPPFRS are used as control groups in the actual application effect test of Gabor-ML-LPP-based station passenger FRS. The results of the average absolute error and the maximum absolute percentage error of the three FRSs as a function of the number of iterations are displayed in Figure 10.

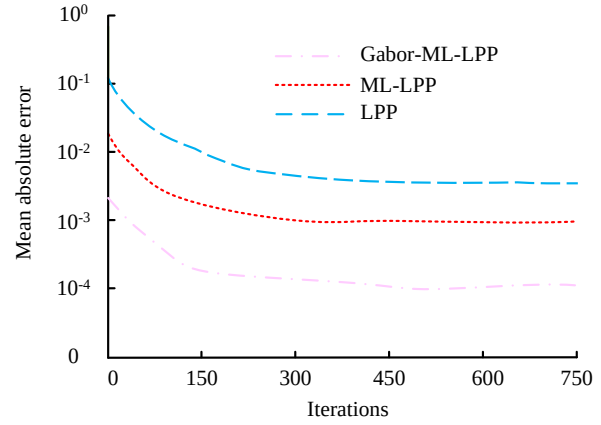

(a) Mean absolute error

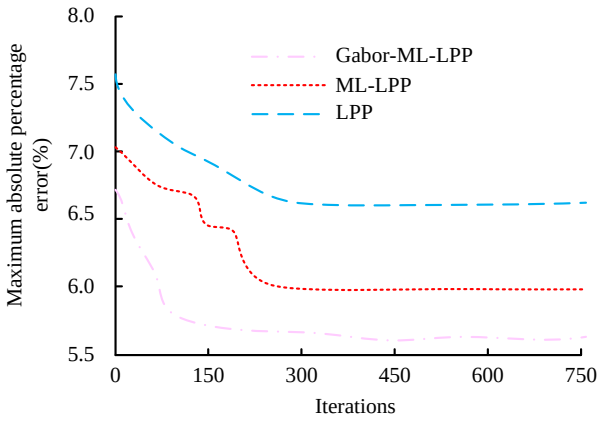

(b) Maximum absolute percentage error

Figure 10: Mean absolute error and maximum absolute percentage error

From Figure 10(a), the average absolute error of Gabor-ML-LPP system is stable at 1.14-4, ML-LPP system is stable at 1.99-4, and LPP is stable at 2.51-4 after 750 iterations of operation. In Figure 10(b), the maximum absolute percentage error of Gabor-ML-LPP is stable at 5.65%, ML-LPP is stable at 5.98%, and LPP is stable at 6.68% after 750 iterations. Based on 10(a) and (b), from the error dimension of FRS, the Gabor-ML-LPP system has the best practical application effect, significantly superior to the face bound system used for comparison. This means that the designed method can be better adapted to long-term operation and more stable. The recognition accuracy of these three systems in the face recognition process varies with the feature dimensions in the face data samples, as shown in Figure 11.

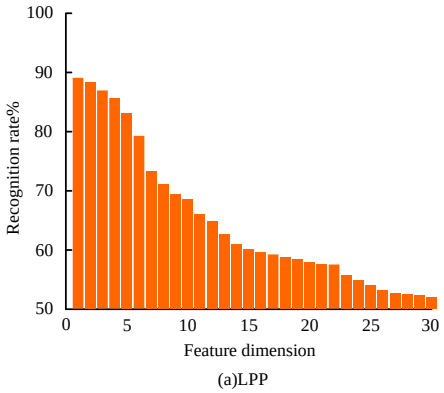

(a)LPP

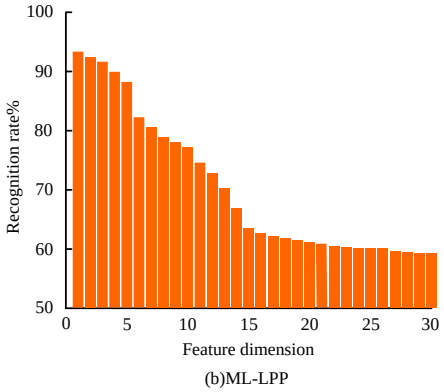

(b)ML-LPP

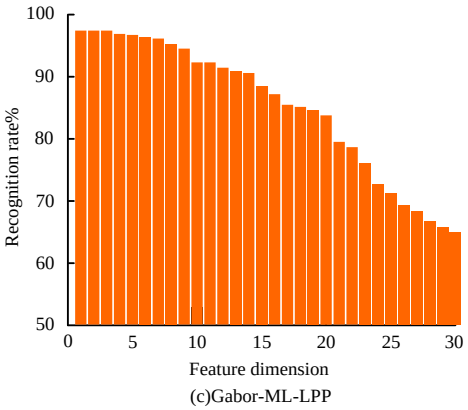

(c)Gabor-ML-LPP

Figure 11: Recognition rates of the different feature dimensions

From Figure 11 (a), the recognition accuracy of the LPP system continuously decreases with the increasing dimension of sample features, from the initial 89% to 52%. From Figure 11(b) and Figure 11(c), the ML-LPP system decreases from the initial 92% to 59%, and the

Gabor-ML-LPP system decreases from 98% to 66%. Based on Figures 11(a), (b), and (c), the accuracy of the three types of FRS decreases with the increase of sample feature dimensions. Among them, Gabor-ML-LPP not only has the highest initial recognition rate, but also has the strongest ability to resist the adverse effects of dimensional changes, which is superior to the comparison system. The above results show that the designed system can identify passengers more accurately, reduce false detection and missing detection, and improve the efficiency of station security and operation. The comparative experiments are conducted on the adaptability of the FRS proposed in the validation study on three datasets: AR, ORL, and YALE. The experimental results are exhibited in Table 3.

Table 3: Recognition rates for the different training sets

Number of training samples	Dataset Type	LPP	ML-LPP	Gabor-ML-LPP
5	AR	77.19%	88.11%	96.77%
	ORL	75.12%	85.17%	95.12%
	YALE	76.88%	82.55%	97.18%
7	AR	70.23%	84.13%	93.51%
	ORL	69.15%	81.74%	92.88%
	YALE	69.16%	80.85%	93.22%
9	AR	60.32%	79.81%	91.14%
	ORL	62.99%	77.63%	91.02%
	YALE	61.77%	79.66%	90.55%

From Table 3, using AR dataset for comparative experiments, when the number of training samples is 5, 7, and 9, the recognition rates of LPP are 77.19%, 70.23%, and 60.32%. The ML-LPP values are 88.11%, 84.13%, and 79.81%. Gabor-ML-LPP has 96.77%, 93.51%, and 91.14%. Comparative experiments are conducted using the ORL dataset. When the number of training samples is 5, 7, and 9, the recognition rates of LPP are 75.12%%, 69.15%, and 62.99%. The rate of ML-LPP is 85.17%, 81.74%, and 77.63%. The rate of Gabor-ML-LPP is 95.12%, 92.88%, and 91.02%. Using the YALE dataset for comparative experiments: When the number of training samples is 5, 7, and 9, the LPP series is 76.88%, 69.16%, and 61.77%, ML-LPP is 82.55%, 80.85%, and 79.66%, and Gabor-ML-LPP is 97.18%, 93.22%, and 90.55%. The Gabor-ML-LPP system has the highest recognition rate on these three datasets, and the recognition rate is least affected with the increase of training samples. In summary, the practical application effect of the Gabor-ML-LPP-based station travel FRS proposed in the study is better than that of the comparative system, proving the reliability and practicality of the design system.

5 Conclusion

In recent years, the passenger flow at stations has gradually increased, especially during holidays, and the pressure on station security work is enormous. To improve the efficiency of security checks, stations are gradually using FRS for security checks. However, when traditional FRS is implemented in stations, its recognition accuracy is not high. In response to this issue, the study proposed to improve traditional face recognition algorithms using GW and ML, and to construct station passenger FRS based on the improved algorithm. Performance comparison experiments were conducted on the improved algorithm. The results showed that the recognition accuracy of the algorithm was 97%, and the area under the accuracy recall curve was 0.87. After 200 iterations of the algorithm, its accuracy and loss values remained stable at 94% and 0.18 respectively, both better than LPP and ML-LPP. When the number of training samples was 4 or 6, the running time of the algorithm was 2.8 seconds, and the recognition rate ratio was 93% and 912%, both of which were better than the control algorithm. Then the empirical analysis of the practical application effect of the proposed FRS showed that the average absolute error and the maximum absolute percentage error of Gabor-ML-LPP system were 1.14-4 and 5.65%.These data were better than the comparison system. Compared to the comparison system, the recognition accuracy of this system decreased the least for different sample feature dimensions. When the system was compared and tested on different datasets, its recognition rate was higher than that of the comparative FRS. In summary, the proposed GW-ML-based face recognition algorithm and the station passenger FRS constructed based on this algorithm can improve the accuracy of facial recognition in stations. However, the protection function of facial information in this system has not been strengthened, which may lead to information leakage. At the same time, although the running time of the algorithm is shorter, the requirement for real-time performance may be higher in the high-traffic station environment. Therefore, in the future, the system will explore its data encryption technology to ensure that personal privacy is not compromised, and optimize the algorithm to further reduce the uptime to cope with the demand of peak hours.

Funding

The research is supported by: Zhengzhou Police University 2025 Basic Research Funds for Central Universities Special Fund Project. Analysis of the Current Situation and Optimization Path of Police Enforcement on Trains under the "One Train, One Police" Background. (No. 2025TJJBKY043).

References

[1] Yang, J., He, W., Zhang, T., Zhang, C., Zeng, L., & Nan, B. (2020). Research on subway pedestrian detection algorithms based on SSD model. IET Intelligent Transport Systems, 14(11):1491-1496. https://doi.org/10.1049/iet-its.2019.0806

[2] Yan, H., Wang, P., Chen, W. D., & Liu, J. (2015). Face recognition based on gabor wavelet transform

and modular 2dpca//2015 international conference on power electronics and energy engineering. Atlantis Press, 245-248. https://doi.org/10.2991/peee-15.2015.67

[3] Rashid, S. J., Abdullah, A. I., & Shihab, M. A. (2020). Face recognition system based on gabor wavelets transform, principal component analysis and support vector machine. International Journal on Advanced Science Engineering and Information Technology, 10(3): 959-63. https://doi.org/10.18517/ijaseit.10.3.8247

[4] Khan, I. U., Shah, J. A., Bilal, M., Khan, M. S., Shah, S., & Akgül, A. (2023). Machine learning modelling of removal of reactive orange RO16 by chemical activated carbon in textile wastewater. Journal of Intelligent & Fuzzy Systems, 44(5): 7977-7993. https://doi.org/10.3233/jifs-220781

[5] Khalil, K. (2023). Airline flight delays using artificial intelligence in COVID-19 with perspective analytics. Journal of Intelligent & Fuzzy Systems, 44(4): 6631-6653. https://doi.org/10.3233/JIFS-222827

[6] Otani, Y., & Ogawa, H. (2021). Potency of individual identification of japanese macaques (macaca fuscata) using a face recognition system and a limited number of learning images. Mammal Study, 46(1):85-93. https://doi.org/10.3106/ms2020-0071

[7] Wang, S., Ge, H., Yang, J., & Su, S. (2021). Virtual samples based robust block-diagonal dictionary learning for face recognition. Intelligent Data Analysis, 25(5):1273-1290. https://doi.org/10.3233/IDA-205466

[8] Wang, Z., Abhadiomhen, S., Liu, Z., Shen, X., & Gao, W. (2021). Multi-view intrinsic low-rank representation for robust face recognition and clustering. IET Image Processing, 15(14):3573-3584. https://doi.org/10.1049/ipr2.12232

[9] Chen, T., Gao, T., Li, S., Zhang, X., Cao, J., Yao, D., & Li, Y. (2021). A novel face recognition method based on fusion of LBP and HOG. IET Image Processing, 15(14):3559-3572. https://doi.org/10.1049/ipr2.12192

[10] Sun, R., Shan, X., Zhang, H., & Gao, J. (2022). Data gap decomposed by auxiliary modality for NIR-VIS heterogeneous face recognition. IET image processing, 16(1):261-272. https://doi.org/10.1049/ipr2.12350

[11] Wan, Z., Huang, M., Yang, R., Liu, W., & Zeng, N. (2022). EEG fading data classification based on improved manifold learning with adaptive neighborhood selection. Neurocomputing, 482(14):186-196. https://doi.org/10.1016/j.neucom.2021.11.039

[12] Cui, P., Wang, X., & Yang, Y. (2021). Nonparametric manifold learning approach for improved process monitoring. The Canadian Journal of Chemical Engineering, 100(1):67-89. https://doi.org/10.1002/cjce.24066

[13] Ran, R., Feng, J., Zhang, S., & Fang, B. (2020). A general matrix function dimensionality reduction framework and extension for manifold learning. IEEE Transactions on Cybernetics, 4(52):2137-2148. https://doi.org/10.1109/TCYB.2020.3003620

[14] Dornaika, F. (2020). Multi-layer manifold learning with feature selection. Applied Intelligence, 50(6):1859-1871. https://doi.org/10.1007/s10489-019-01563-9

[15] Duan, Y., Huang, H., Li, Z., & Tang, Y. (2020). Local manifold-based sparse discriminant learning for feature extraction of hyperspectral image. IEEE Transactions on Cybernetics, 51(8):4021-4034. https://doi.org/10.1109/tcyb.2020.2977461

[16] Khan, I. U., & Aftab, M. (2022). Dynamic programming approach for fuzzy linear programming problems FLPs and its application to optimal resource allocation problems in education system. Journal of Intelligent & Fuzzy Systems, 42(4): 3517-3535. https://doi.org/10.3233/JIFS-211577

[17] Khan, I.U., & Rafique, F. (2021). Minimum-cost capacitated fuzzy network, fuzzy linear programming formulation, and perspective data analytics to minimize the operations cost of American airlines. Soft Computing, 25(2): 1411-1429. https://doi.org/10.1007/s00500-020-05228-5

[18] Khan, I. U., & Karam, F. W. (2019). Intelligent business analytics using proposed input/output oriented data envelopment analysis DEA and slack based DEA models for US-airlines. Journal of Intelligent & Fuzzy Systems, 37(6): 8207-8217. https://doi.org/10.3233/JIFS-190641

[19] Khan, I. U., Ahmad, T., & Maan, N. (2019). Revised convexity, normality and stability properties of the dynamical feedback fuzzy state space model (FFSSM) of insulin-glucose regulatory system in humans. Soft Computing, 23: 11247-11262. https://doi.org/10.1007/s00500-018-03682-w

[20] Samantaray, A., & Rahulkar, A. (2020). New design of adaptive Gabor wavelet filter bank for medical image retrieval. IET Image Processing, 14(4):679-687. https://doi.org/10.1049/iet-ipr.2019.1024